Chemosphere 148 (2016) 126–136

Contents lists available at ScienceDirect

Chemosphere

journal homepage: www.elsevier.com/locate/chemosphere

Volatile-organic molecular characterization of shale-oil produced water from the Permian Basin

Naima A. Khan [a], Mark Engle [b], Barry Dungan [a], F.Omar Holguin [a], Pei Xu [a], Kenneth C. Carroll [a, *]

[a] New Mexico State University, Las Cruces, NM, USA
[b] U.S. Geological Survey, El Paso, TX, USA

HIGHLIGHTS

- 1st high-resolution VOC MS data for the shale-oil produced water from Permian.
- Shale-oil water VOC high-resolution GC-ToF-MS identified 1400 compounds.
- 3D van Krevelen and DBE diagrams fingerprinting framework for high-resolution MS.
- Source composition & solubility controlled the composition of the produced water.
- Partial treatment may support beneficial reuse for fracturing or bio-energy.

GRAPHICAL ABSTRACT

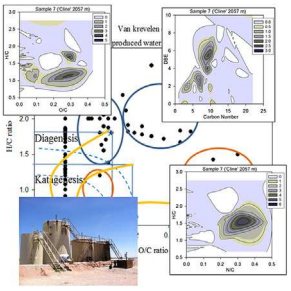

ARTICLE INFO

Article history:
Received 23 September 2015
Received in revised form
23 December 2015
Accepted 27 December 2015
Available online xxx

Handling Editor: Tamara S. Galloway

Keywords:
Produced water
Shale oil
Hydraulic fracturing
Permian Basin
Gas chromatography mass spectrometry
Volatile organic

ABSTRACT

Growth in unconventional oil and gas has spurred concerns on environmental impact and interest in beneficial uses of produced water (PW), especially in arid regions such as the Permian Basin, the largest U.S. tight-oil producer. To evaluate environmental impact, treatment, and reuse potential, there is a need to characterize the compositional variability of PW. Although hydraulic fracturing has caused a significant increase in shale-oil production, there are no high-resolution organic composition data for the shale-oil PW from the Permian Basin or other shale-oil plays (Eagle Ford, Bakken, etc.). PW was collected from shale-oil wells in the Midland sub-basin of the Permian Basin. Molecular characterization was conducted using high-resolution solid phase micro extraction gas chromatography time-of-flight mass spectrometry. Approximately 1400 compounds were identified, and 327 compounds had a >70% library match. PW contained alkane, cyclohexane, cyclopentane, BTEX (benzene, toluene, ethylbenzene, and xylene), alkyl benzenes, propyl-benzene, and naphthalene. PW also contained heteroatomic compounds containing nitrogen, oxygen, and sulfur. 3D van Krevelen and double bond equivalence versus carbon number analyses were used to evaluate molecular variability. Source composition, as well as solubility, controlled the distribution of volatile compounds found in shale-oil PW. The salinity also increased with depth, ranging from 105 to 162 g/L total dissolved solids. These data fill a gap for shale-oil PW composition, the associated petroleomics plots provide a fingerprinting framework, and the results for

* Corresponding author.
E-mail address: kccarr@nmsu.edu (K.C. Carroll).

http://dx.doi.org/10.1016/j.chemosphere.2015.12.116

the Permian shale-oil PW suggest that partial treatment of suspended solids and organics would support some beneficial uses such as onsite reuse and bio-energy production.

1. Introduction

Produced water (PW), as the largest waste stream generated during oil and gas production, is a mixture of formation water naturally present in reservoirs and water injected into reservoirs for pressure support, hydraulic fracturing, or reservoir treatment (Veil et al., 2004; Ahmadun et al., 2009). Understanding the sources and chemistry of formation waters is critical in oil-field management and petroleum exploration for many reasons such as planning for saltwater disposal and secondary recovery projects, proper treatment of production fluids to prevent corrosion and enhance phase separation (Ostroff, 1979). Also, predicting and locating variations in PW quality supports evaluating potential beneficial uses and treatment needs (Ahmadun et al., 2009).

Recent advances in horizontal drilling and hydraulic fracturing have caused a significant increase in unconventional hydrocarbon production including shale gas, coal-bed methane, tight oil, oil sands, and shale oil (Alley et al., 2011; Maguire-Boyle and Barron, 2014). Alley et al. found that PW compositions vary between each conventional and unconventional hydrocarbon production formation types (Alley et al., 2011). Orem et al. found that PW can be significantly altered from that of the formation for up to 250 days after hydraulic fracturing due to influence from compounds added during hydraulic fracturing (Orem et al., 2014), and Rowan et al. observed hydraulic fracturing flowback in PW from shale gas for up to 90 days (Rowan et al., 2015). Although compositions are highly variable, PWs contain dissolved inorganic salts (e.g. sodium, chloride, etc.), chemical additives used for drilling and well operations (e.g., hydraulic fracturing and/or corrosion inhibitor, biocide, and friction reducers), dissolved oil components (e.g. petroleum compounds), naturally occurring radioactive materials, suspended solids, and dissolved gases (Veil et al., 2004; Silset et al., 2010).

Several researchers have examined, to some extent, the organic composition within PW from various formations around the world (Utvik, 1999; Faksness et al., 2004; Sirivedhin and Dallbauman, 2004; Tellez et al., 2005; Lu et al., 2006; Dorea et al., 2007; Silset et al., 2010; Horner et al., 2011; Wang et al., 2012; Eftekhardadkhah and Oye, 2013; Maguire-Boyle and Barron, 2014; Orem et al., 2014). The composition and volume of PW varies as a function of the geologic formation and the age of the field (Dudasova et al., 2009). Tellez et al. used gas chromatography–mass spectroscopy (GC–MS) to evaluate PW from Permian Basin (Tellez et al., 2005). This work was conducted prior to the vast increases in unconventional oil production in the Permian, and there are no previously published investigations of PW from tight oil reservoirs within the Permian Basin, which is the most productive tight oil play in the US (Guerra et al., 2011). Recently, production in the Permian Basin has been >2 million barrels of oil per day (U.S.E.I.A., 2015). Despite use of GC–MS in several of these prior studies, the reported results focused on bulk trends in organic composition or on select compounds that could be separated and quantified. Wang et al. was the only paper that did use high-resolution MS and examined the complex mixture within PW from a conventional oil field in Wyoming using petroleomics analysis approaches including van Krevelen and double-bond equivalent (DBE) versus carbon number plots (Wang et al., 2012).

High-resolution GC–MS is critical for detailed organic-compositional fingerprinting and characterization of hydrocarbon mixtures. Gas chromatography-time of flight-mass spectroscopy (GC-ToF-MS) and Fourier transform ion cyclotron resonance mass spectrometry (FT-ICR-MS) are two of the few instruments that have been able to resolve the thousands of compounds in both crude oil and shale oil (Stanford et al., 2007; Avila et al., 2012; Cho et al., 2012, 2013; Jin et al., 2012; Kekalainen et al., 2013; Lababidi et al., 2013). The majority of this work used FT-ICR-MS for hydrocarbon analysis, whereas GC-ToF-MS has not been used as much even with its high-resolution capability for low polarity and nonpolar organic mixtures. Moreover, results plotted in van Krevelen diagrams have been typically used for oil maturation and source comparison (Kim et al., 2003; Wu et al., 2004), and they also appear well suited to amplify and expose compositional differences within and between complex organic mixtures such as PWs.

Despite prior work, there is still vast uncertainty in the molecular-level composition of PWs derived from unconventional hydrocarbon production formations. To our knowledge, no organic composition data are available from the unconventional shale-oil PW being produced from the Permian Basin or other shale-oil plays (Eagle Ford, Bakken, etc.). The goal of this study was to characterize the volatile organic compositional variability of late stage shale-oil PW from the Permian Basin using high-resolution GC–MS. Late stage PW, generally collected months or years after wells go into production is more indicative of the native formation water (Rowan et al., 2015), as opposed to analysis of early stage and flowback PW, which is particularly focused on the compounds used for hydraulic fracturing. Injected fracturing compounds are already reported for all wells in Texas through the FracFocus database. The organic compositional data for the PW samples was compared to the organic composition of oil and shale oil. Comparison of PWs quality with standards for drinking water was also used to examine beneficial use and treatment options.

2. Materials and methods

2.1. Permian Basin hydrogeology

The Permian Basin province, containing multiple sub-basins located in western Texas and eastern New Mexico, is one of the most productive hydrocarbon plays within North America, containing conventional oil, tight oil, and natural-gas resources (Guerra et al., 2011). Due to the depositional history, there are significant variations in lithology, geochemistry, and hydrologic properties of the hydrocarbon reservoirs. Fig. 1 presents the stratigraphic column of Midland Basin within the Permian Basin with the lithologic setting. At their deepest points the two sub-basins, the Midland and Delaware Basins, contain approximately 4600 m and 10,700 m of sediments, respectively, overlying Precambrian basement. Pre-Pennsylvanian strata that consist primarily of those contained in the precursor to the Permian Basin, the Tobosa Basin, are composed of marine carbonates and shales. Permian-age sediments include a sequence of geologic strata including evaporites, carbonates, discontinuous fluvial-deltaic arkosic sandstones, very fine siltstone and marine shales (Fig. 1). Historically, much of the hydrocarbon production was derived from conventional structural and stratigraphic traps in Guadalupian and Leonardian age reservoirs

Era	Period	Time (Ma)	Epoch/Era	Midland Basin	Lithology
Paleozoic	Permian	251	Ochoan	Dewey lake	Halite, Anhydrite, & Sylvite
				Rustler	
				Salado	
					Sandstone & Anhydrite
			Guadalupian	Tansil	
				Yates	
				Seven Rivers	
				Queen	
				Grayburg	
				San Andres	Dolomite
				Brushy Canyon	Limestone & Dolomite
			Leonardian		
				Spraberry	
				Dean	
			Wolfcamp	Wolfcamp	Limestone & Shale
	Pennsylvanian	302	Virgil	Cisco or 'Cline'	
			Missourian	Canyon	
			Des Moines	Straw	
			Atoka	Atoka	Shale
		323			

Fig. 1. Generalized stratigraphy of the Paleozoic Era across the Permian Basin [Modified from Bassett and Bentley and Dutton et al. (1982, 1987)].

(Dutton et al., 2005). More recently, with the advent of horizontal drilling and slick water hydraulic fracturing, low permeability, organic-rich source rocks in the Leonardian (e.g., Spraberry, Bone Spring, Avalon, etc.), Wolfcampian (i.e., Upper, Middle, and Lower Wolfcamp shales), and Pennsylvanian (e.g., "Cline" shale) age reservoirs have been targets for production. Above the hydrocarbon-bearing reservoir rocks of the Permian Basin, there is an evaporite layer (primarily anhydrite and halite) overlain by fluvial, deltaic, and lacustrine deposits of the Triassic Dockum Group and the Neogene Ogallala (Senger et al., 1987). Geochemical investigation of PWs, particularly those thought to represent the native formation brines present in the reservoirs prior to hydrocarbon production, can provide a broad spectrum of information about the history, origin, and geology of the basin and its fluids. Recent work by Engle and Blondes (Engle and Blondes, 2014) has evaluated the brine geochemistry of the Guadalupian-age Permian Basin formations. Thus, PW brine chemistry is not discussed herein.

2.2. Sample collection

PW samples were collected from oil-producing wells in Texas (i.e., Midland Basin). The PW samples were collected from 8 different wells that were producing from the Wolfcamp Shale Formation, except for sample 1 which had a producing depth that extended into the 'Cline' Shale Formation below the Wolfcamp (Table 1). The total thickness of the stratigraphic subset sampled and examined for this study was 1892–2163 m below land surface of the Midland sub-basin of the Permian Basin. All samples had average temperature of 31 °C, and pH was 8 on average. There were 6 samples collected directly from the wellhead, and 2 samples were collected from the oil-water separators adjacent to the wellhead. Samples were collected during production approximately 130–441 days after hydraulic fracturing, and thus they tend to represent the native formation waters rather than compounds involved with hydraulic fracturing. Samples were collected without any headspace in 4-L amber glass volatile organic analysis (VOA) vials, which were previously washed with distilled-deionized water and oven dried. Additional sampling, including replicates, to support an ongoing inorganic and isotopic chemistry investigation was also conducted.

2.3. Chemical analysis

All samples were refrigerated at 4 °C (<1 month), and then placed on a bench top for 24 h to settle suspended solids and oil droplets prior to sampling. Then a 10 mL pipette was used to collect samples from the water phase. Dilution (10×) with distilled-deionized nanopure (Series 550, Barnstead Thermolyne Corp., Dubuque, Indiana) water was required to meet the linear analysis response range. A standard mixture of benzene, toluene, ethylbenzene and xylene (BTEX) and fifteen other volatile compounds (Chem Service, Inc; model # VOC-1N; Serial # 93-112778) with a concentration of 20 mg/mL of each component was prepared from the pure analytes by weight in methanol (Merk, Darmsradt, Germany). A 1 mg/L standard solution of BTEX and fifteen other volatile compounds was prepared from the pure analytes (Merck). Finally, 20 μL Anthracene-D10 (Restek, Catalog # 31037) was spiked in 1 mg/L standard solution as internal standard, which was used for calculating response factors of those standard chemicals.

A CTC Analytics (Switzerland) CombiPAL autosampler fitted with a 100 μm polydimethylsiloxane (PDMS) solid phase micro extraction (SPME) fiber was used to collect and deliver samples. Each sample was incubated for 5 min at 45 °C, and then sampled for 5 min. After sampling, the fiber had a 10 min desorption time in the injector, which was fitted with a septaless Merlin Microseal. For analyzing organic compounds in PW, GC-ToF-MS was used with a modified Petroleum Refinery Reformate method. Injections were made on a 7890A Agilent Gas Chromatograph fitted with a ZB-5MS column (30 m, 0.25 mm I.D., 0.25 μm film thickness) with helium as the carrier gas. A solvent delay of 0.1 min was used. The inlet was in splitless mode with a constant flow of 0.6 mL/min for the entire run, and a front inlet septum purge of 3 mL/min. The inlet was operated at a constant 225 °C and the transfer line was constant at 275 °C. The oven program started at 35 °C, held for 4 min, ramped to 110 °C at 5 °C/minute, ramped to 280 °C at 7 °C/minute, and held for 0.5 min. A Leco Pegasus High Throughput Time of Flight Mass Spectrometer detector was used for all GC–MS analyses. We collected masses from 55 to 550 m/z with an acquisition rate of 20 spectra/second operating at 1800 V, and the ion source was heated at 210 °C. ChromaTof version 4.41 was used for data processing with automatic smoothing, 1.5 s peak width, baseline subtraction just through the middle of the noise, and automatic mass spectral deconvolution and peak detection at 100:1 signal to noise ratio.

Subsamples from the 8 samples were mixed uniformly (5 mL from each sample) into 40 mL. Then 5 mL subsample of that mix was diluted with 5 mL of nanopure water in 20 mL SPME vials spiked with Anthracene-D10, which was then analyzed with GC-ToF-MS for creating an Ion file assumed to be representative for all samples. This Ion file was used for aligning all ions in all PW samples in a common file with Met Idea software. Then the compounds with 70%, or greater, match to the National Institute of Standard and Technology (NIST) library were considered for the

Table 1
Produced water sample summary and analysis results for total dissolved solids (TDS), total suspended solids (TSS), total organic carbon (TOC), and dissolved organic carbon (DOC).

Sample ID	Sedimentary formation	Sampling location	Sample time after fracturing (days)	Sample depth (meter)	TDS (mg/L)	TSS (mg/L)	TOC (mg/L)	DOC (mg/L)
Sample 1	Wolfcamp	Wellhead	151	1892	106,540	6850	86.25	63.45
Sample 2	Wolfcamp	Separator	412	1914	113,760	16,330	123.71	127.09
Sample 3	Wolfcamp	Wellhead	403	1928	116,370	7410	173.33	145.71
Sample 4	Wolfcamp	Wellhead	366	1972	105,030	9110	90.6	82.83
Sample 5	Wolfcamp	Wellhead	411	1978	119,083	12,060	164.34	98.27
Sample 6	Wolfcamp	Wellhead	418	2055	114,830	18,720	139.74	112.11
Sample 7	Cline	Wellhead	441	2057	162,880	20,560	142.84	99.8
Sample 8	Wolfcamp	Separator	130	2163	142,630	21,820	184.21	139.66

rest of the analysis. Response factors for all standards with the internal standards were calculated as the ratio of the product of the compound area and internal standard concentration divided by the product of the internal standard area and compound concentration. The response factors were used for calculating concentration and relative concentration of organic compounds in PW samples. Peak abundances for all compounds were normalized based on the anthracene-D10 peak area, and then the abundance of the internal standard peak was used to normalize the abundance of other peaks (Cho et al., 2013). A surrogate for concentration, relative abundance was determined for all compounds not included in the volatile compound external standard mixture (Chem Service, Inc; model # VOC-1N; Serial # 93-112778). The relative abundance of each individual compound was calculated as the normalized peak area divided by the sum of all normalized peak areas (as %). Double bond equivalence (DBE) represents the number of rings plus the number of double bonds in a given molecular formula. DBE values were calculated using Equation (1) from Cho et al. (2013).

Total solids (TS), total dissolved solids (TDS), and total suspended solids (TSS) were measured gravimetrically after heating in an oven (VWR-1370 FM). Standard Methods 2540 C method was used for TDS measurement. Total Organic Carbon Analyzer (Simadzu TOC-L, Kyoto, Japan) was used for analyzing total carbon and inorganic carbon in each PW sample. Samples were centrifuged before measurement of total organic carbon (TOC) and filtered by 0.45 μm cellulose acetate membrane (Toyo Roshi Kaisha, Ltd., Japan) before measurement of dissolved organic carbon (DOC). Subsamples were filtered and preserved with 2% nitric acid before inductively coupled plasma-optical emission spectrometer (ICP-OES) cation analysis, and anions were evaluated with ion chromatography and technical auto analyzer (data not shown). Acumen pH/Specific Ion Meter Model 25 was used for measurements of bicarbonate and alkalinity by titration (Franson, 1992).

3. Results and discussion

3.1. Produced water quality

The results of late stage shale-oil PW sampling and analysis from the shale-oil producing units in the Permian fill an important data gap for organic composition data, which to our knowledge have not previously been available for unconventional shale-oil PW being produced from the Permian Basin or other important shale-oil plays (Eagle Ford, Bakken, etc.), which have experienced tremendous production increases recently due to hydraulic fracturing. The shale-oil PWs samples exhibited significant compositional variability, and generally elevated (compared to fresh water and most shallow groundwater used for hydraulic fracturing) concentrations of salts and organic compounds (Table 1). Fresh groundwater was used for hydraulic fracturing, and flowback after fracturing is a mixture of fresh water and formation brine until flowback has been removed and only formation water remains in the PW. TDS values in Table 1 are all approximately a factor of 3 larger than sea water, and they are generally higher than the diluted PW observed during fracturing flowback, which suggests that the samples are representative of the formation and not impacted by fracturing operations. This was confirmed by examination of replicate sample isotope results (data not shown). Fig. 2 presents TDS, TSS, DOC, and TOC as a function of formation depth below land surface, which generally indicates increasing values for each parameter with depth over the section investigated. The sampled shale-oil PWs had a large salinity (TDS) range of 105–162 g/L, and concentrations of TOC and DOC were less variable. The mean values for TDS, TSS, TOC, and DOC were 122,640, 14,107, 138, 109 mg/L, respectively. Sirivedhin and Dallbauman (2004) measured the DOC range of 9–13 mg/L for oil-PW from Oklahoma, and Wang et al. (2012) measured 15 mg/L DOC for oil-PW from Wyoming. TOC values reported for PW from shale-gas can be significantly higher than the values reported from this study, and TOC values for coal bed methane PW are typically lower than those we report for shale-oil PW (Maguire-Boyle and Barron, 2014; Orem et al., 2014). Many oil-formation PWs typically have TDS values up to 1 or 2 g/L (Dorea et al., 2007; Horner et al., 2011), whereas Sirivedhin and Dallbauman (2004) reported >70–100 g/L for the range of oil-PW TDS values. The known range for TDS of PWs in Permian basin is ~100–300 g/L (Guerra et al., 2011). These results suggested that PW derived from the oil-bearing shale formations were sourced from partially evaporated paleo-seawater while PW derived from shallower formations consist of meteoric water that dissolved halite and anhydrite (Engle and Blondes, 2014).

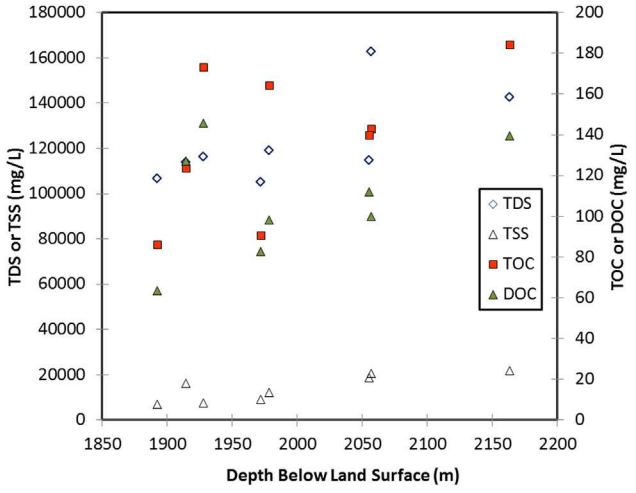

Fig. 2. Comparison of total dissolved solids (TDS), total organic carbon (TOC), and dissolved organic carbon (DOC) as a function of depth below land surface.

3.2. Quantitative organic composition

Approximately 1400 organic chemicals were identified with peak separation and deconvolution, and approximately 300–400 of these compounds had identifiable structures. These results suggest that PW from oil-bearing shale formations may be one of the most complex mixtures identified in water, and that there is a vast suite of volatile and semi-volatile organic compounds that dissolve into water from shale-oil formations. Even though many had uncertain structures, there were 327 compounds with structures identified with confidence (70% or greater match with NIST library), which were extracted by processing chromatograms with Met-Idea software by aligning all ions in a common file. The Anthracene-D10 spike was used to quantify relative abundance for the 327 compounds in each of the samples. Detection of volatile organic compounds by SPME is impacted by the "salting-out effect" where the transfer to gas from aqueous phase becomes increased by increasing the ionic strength of the aqueous phase (Lambropoulou and Albanis, 2001). Generally, the addition of salt is thought to increases the sensitivity of the hydrophobic compounds, and the extraction and detection of volatile organic compounds was most likely enhanced for PW samples compared to fresh water samples.

A subset of the 327 compounds was evaluated using the internal and external standards for quantification of aqueous concentration. Table 2 presents eight identified compound classes in the shale-oil PWs along with their concentration, which included the BTEX compounds that are typically considered for health and toxicity concerns. These results illustrate the compositional variability observed within shale-oil PW. For example, the concentration range for benzene nearly spans 3 orders of magnitude, and even the mean concentration of 107 mg/L for benzene is greater than four orders of magnitude higher than the maximum contaminant level (MCL) for drinking water in the U.S. Reported benzene composition within PW from oil-formations varies in the range of 1–4 mg/L (Utvik, 1999), 0.03–0.1 mg/L (Sirivedhin and Dallbauman, 2004), 1.4 mg/L (Dorea et al., 2007), and 0.026 mg/L (Horner et al., 2011), which are 1–4 orders of magnitude lower than the mean reported here for shale-oil PW. Although these compounds are generally considered volatile and biodegradable, their toxicity suggests that treatment of these chemicals may be required prior to many of the potential beneficial use or reuse alternatives (Veil et al., 2004; Xu et al., 2008a, 2008b; Graham et al., 2015).

3.3. Hydrocarbon classes

Most oil and gas PWs primarily contain cyclohexane, cyclopentane, alkanes, polyaromatic hydrocarbons, and heteroatomic compounds (Orem et al., 2014). The most prevalent group in shale-oil PW is straight chain alkanes based on the Permian Basin shale-oil PW samples evaluated herein. Fig. 3 presents relative abundance of hydrocarbon classes (cyclohexane, cyclopentane, n-alkanes) from lower to higher concentration trend (i.e., relative abundance) for each of the shale-oil PW samples from the Permian Basin. Among all hydrocarbons, straight chain alkanes (C_nH_{n+2}) are the major compound class contributing to the TOC (Fig. 3) from all samples examined in this study though their relative abundance did exhibit a wide range of variability. Alkanes were also found as the most dominant organic group in a PW sample from a prior study conducted in the Permian Basin (Tellez et al., 2005). The trend observed in Fig. 3 was also comparable to the results published on oil-gas cuts [petroleum oil fraction obtained by molecular distillation from crude oil]. For example, Avila et al. also found the same trend, and comparable relative concentrations, for oil-gas cuts (Avila et al., 2012). This suggests that source-oil composition has a significant impact on PW hydrocarbon composition.

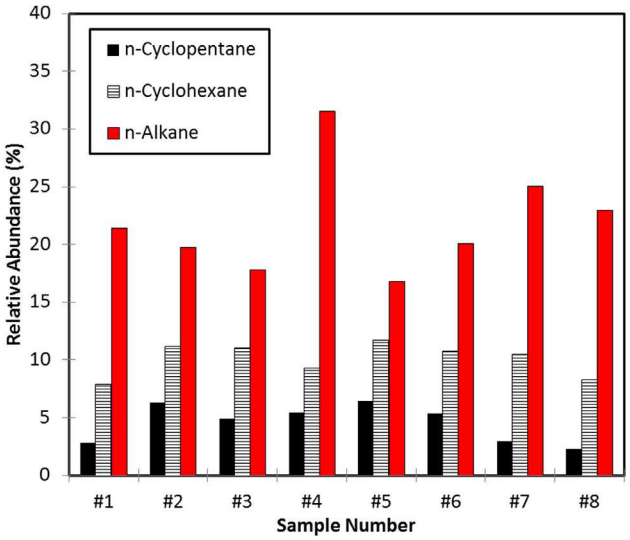

Fig. 3. Comparison of alkane, cyclohexane and cyclopentane relative abundance in PW samples. The sample numbers are ordered by increasing depth from left to right.

Both alkanes and heteroatomic hydrocarbon groups have been identified within the shale-oil PW samples from the Permian Basin. Among all heteroatomic compounds detected and matched, nitrogen and oxygen containing hydrocarbons are dominant, and only two sulfur-containing compounds had a structure match (>70%). However, many other sulfur, nitrogen, and oxygen containing compounds have been identified with a <70% library match.

Table 2
Summary of benzene, toluene, ethylbenzene, and xylene (BTEX) compound concentrations (mg/L) and statistics.

Sample ID	Alkyl propo-benzene	Alkyl benzene	Chloro-benzene	Alkyl naphthalene	BTEX			
					Benzene	Toluene	p-Xylene	Ethylbenzene
Sample 1	9.34	74.63	0.02	0.67	1.50	0.11	0.02	2.01
Sample 2	38.12	427.80	0.10	1.12	8.93	0.67	0.25	28.11
Sample 3	13.45	130.63	0.04	0.38	5.87	0.41	0.05	7.94
Sample 4	209.15	5092.60	0.03	4.20	778.51	5.61	0.01	399.84
Sample 5	79.77	917.80	0.19	1.32	45.55	3.03	0.46	81.78
Sample 6	35.80	384.88	0.04	1.13	6.25	0.46	0.14	27.87
Sample 7	94.59	1751.03	0.35	1.68	7.82	2.12	0.25	29.18
Sample 8	14.97	175.43	0.04	1.15	4.14	0.10	0.03	4.12
Average	61.90	1119.35	0.10	1.46	107.32	1.56	0.15	72.61
Minimum	9.34	74.63	0.02	0.38	1.50	0.10	0.01	2.01
Maximum	209.15	5092.60	0.35	4.20	778.51	5.61	0.46	399.84
Standard deviation	67.22	1698.91	0.11	1.18	271.57	1.94	0.16	134.63

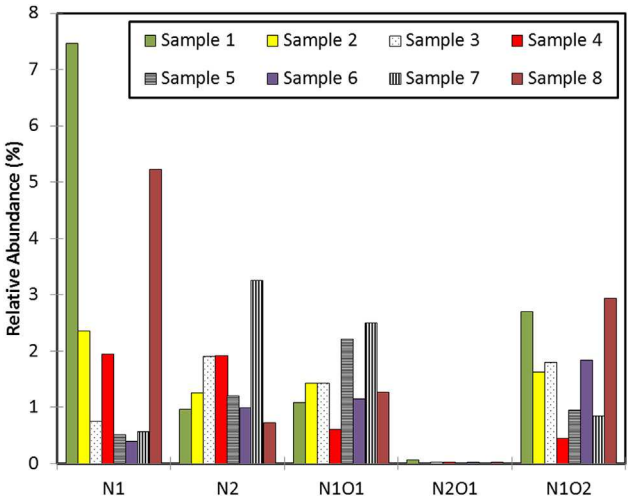

Fig. 4. Comparison of heteroatomic compound class as relative abundance in PW samples. The sample numbers are ordered by increasing depth from left to right.

Fig. 4 presents the relative abundance of heteroatomic compounds as a function of the chemical classes for each of the shale-oil PW samples. Overall, the N_1, N_2 and N_1O_1 classes were more abundant compared to N_3, N_3O_1 classes, which was also the same trend observed in oil-shale pyrolysates chemical analysis (Jin et al., 2012; Cho et al., 2013). This observation suggests that shale-oil PW and oil-shale pyrolysates have similar heteroatom compositions, which supports the observation that source-oil composition has a significant impact on PW composition. The comparison of source oil and PW composition may be especially favorable for heteroatom compounds, which tend to be more polar and soluble. An exception in this comparison is observed for N_2O_1 and N_1O_2. For the PW results, N_2O_1 is less than N_1O_2 whereas, in shale oil composition, N_1O_2 was less than N_2O_1 containing compounds. This discrepancy may be analytical, because electrospray ionization FT-ICR-MS is more sensitive for detection of polar compounds compared to GC-ToF-MS (Zhou et al., 2012).

3.4. Van Krevelen analysis

Van Krevelen diagrams, cross-plots of atomic hydrogen:carbon (i.e., H/C) as a function of oxygen:carbon (i.e., O/C) for all the measured hydrocarbons, can be used for hydrocarbon thermal maturation evaluation, and may also support organic mixture characterization and forensic analysis. The analysis for the shale-oil PW samples from the Permian Basin suggests both Type I (Lacustrine) and Type II (Marine) source rock, and it also suggests diagenetic source-rock alteration supported shale-oil formation. This is reasonable for the Wolfcamp, because there has been almost complete conversion of smectite to illite, suggesting that clay mineral diagenesis was nearly complete. For the van Krevelen evaluation presented herein, H/C was plotted both as a function of O/C and N/C, and comparison of concentration variability was examined by addition of contours of relative abundance. These plots compare the alkene to heteroatomic abundance distribution. Progression to increased H/C and N/C values follows with increasing degree of unsaturation (Cho et al., 2013).

Fig. 5 contains the 3D van Krevelen diagrams for each of the shale-oil PW samples with O/C on the x-axis and relative abundance (%) contours. Comparison of these figures suggests that there are significant deviations between the overall magnitude of volatile organic compound abundance, or concentration, as confirmed by the change in the plot scales, and spatial patterns within the figures confirm the variability between samples for the spectrum of compound abundances. Despite these observations, there are similarities and trends that can be detected. The overall range of abundance generally increases with depth until the two deepest samples.

There are several peaks and areas of elevated abundance compared to the background. Table 3 lists the names and formulas of the major abundance peak compounds observed in the van Krevelen diagrams. There is an abundance peak at H/C 1.2 and O/C 0.1 present in samples 1, 2, 3, 5, 6, 7, and 8 (missing from 4), which is 1-(2,4-dimethylphenyl)-ethanone ($C_{10}H_{12}O$). There is another area of abundance observed in three of the deeper samples (i.e., 5, 6, and 7), that covers H/C 1–1.4 and O/C 0.15–0.4, which is represented by compounds such as 1-(2-furanyl)-3-butene-1,2-diol ($C_8H_{10}O_3$). Another peak at H/C 1.7 and O/C 0.3 is not present in any of the samples except the two deepest samples (i.e., 8 and 7), which is acetyl valeryl ($C_7H_{12}O_2$). These results are similar to the van Krevelen results for PW from conventional oil production in Wyoming, which ranged from H/C 0.5–2.4 and O/C 0–0.8 (Wang et al., 2012). Wang et al. also noted that the peak at H/C 1.2 and O/C 0.1 tended to be condensed hydrocarbons, and lipids occur at H/C ~1.8 and O/C ~0.2.

Fig. 6 presents the 3D van Krevelen diagrams for each of the PW samples with N/C on the x-axis and relative abundance (%) contours. As was observed from the O/C plots, the N/C plots also illustrate the compositional variability and complexity of the shale-oil PW samples, and there is also a trend of increasing abundance with depth. One prominent feature is the abundance peak around H/C of ~1.7 and N/C of ~0.3. This peak increases in size and abundance with depth and varies based on compositional fluctuations of compounds such as butanenitrile (C_4H_7N), cyanic acid propyl ester (C_4H_7NO), and 1,4-dimethyl-2,3-diazabicyclo[2.2.1]hept-2-ene ($C_7H_{12}N_2$). The efficacy of Figs. 5 and 6 for characterizing trends in such complex mixtures suggests that petroleomics fingerprinting methods such as 3D van Krevelen plotting can be used to characterize PW from oil and gas production including shale-oil.

3.5. Double bond equivalence analysis

Fig. 7 presents the 3D cross-plots of DBE as a function of carbon number with relative abundance (%) contours for each of the PW samples. As was observed from the 3D van Krevelen diagrams, the 3D DBE plots also illustrate the compositional variability and complexity of the shale-oil PW samples. However, the DBE plots focus primarily on the aromaticity of conjugated cycloalkenes within the mixtures. It is also evident from these plots that a number of peaks in abundance can be observed, and Table 3 also listed the names of the peak compounds. The area of abundance within plots for samples 1 and 3 along the upper border is typical for multi-ring polycyclic aromatic hydrocarbons (PAHs) such as phenanthrene (i.e., $C_{14}H_{10}$). The two neighboring peaks in the center of the sample 3 plot at DBE 7 – C 11 and DBE 7 – C 14 are represented by 2-methyl-naphthalene ($C_{11}H_{10}$) and 1,4,5,8-tetramethylnaphthalene ($C_{14}H_{16}$), respectively. Another peak, just below at DBE 4 or 5 – C 10 is represented by 1-methyl-3-propyl-benzene ($C_{10}H_{14}$) and 1-(2,4-dimethylphenyl)-ethanone ($C_{10}H_{12}O$). The peak at DBE 2 – C 4, butanenitrile (C_4H_7N), is missing from sample 6 and prominent in samples 1, 2, 4, 5, 7, and 8. This peak is adjacent to another peak in samples 5 and 7, but they are separated by a difference in carbon number. This other peak is located at DBE 2 – C 7, which is represented by 3-methylcyclohexene (C_7H_{12}). In deeper samples 3, 4, 5, and 7, additional peaks at DBE 3 – C 6 and DBE 4 - C 6 develop, which are due to 2-methoxyfuran ($C_5H_6O_2$) and benzene C_6H_6. These results are similar to the DBE results for

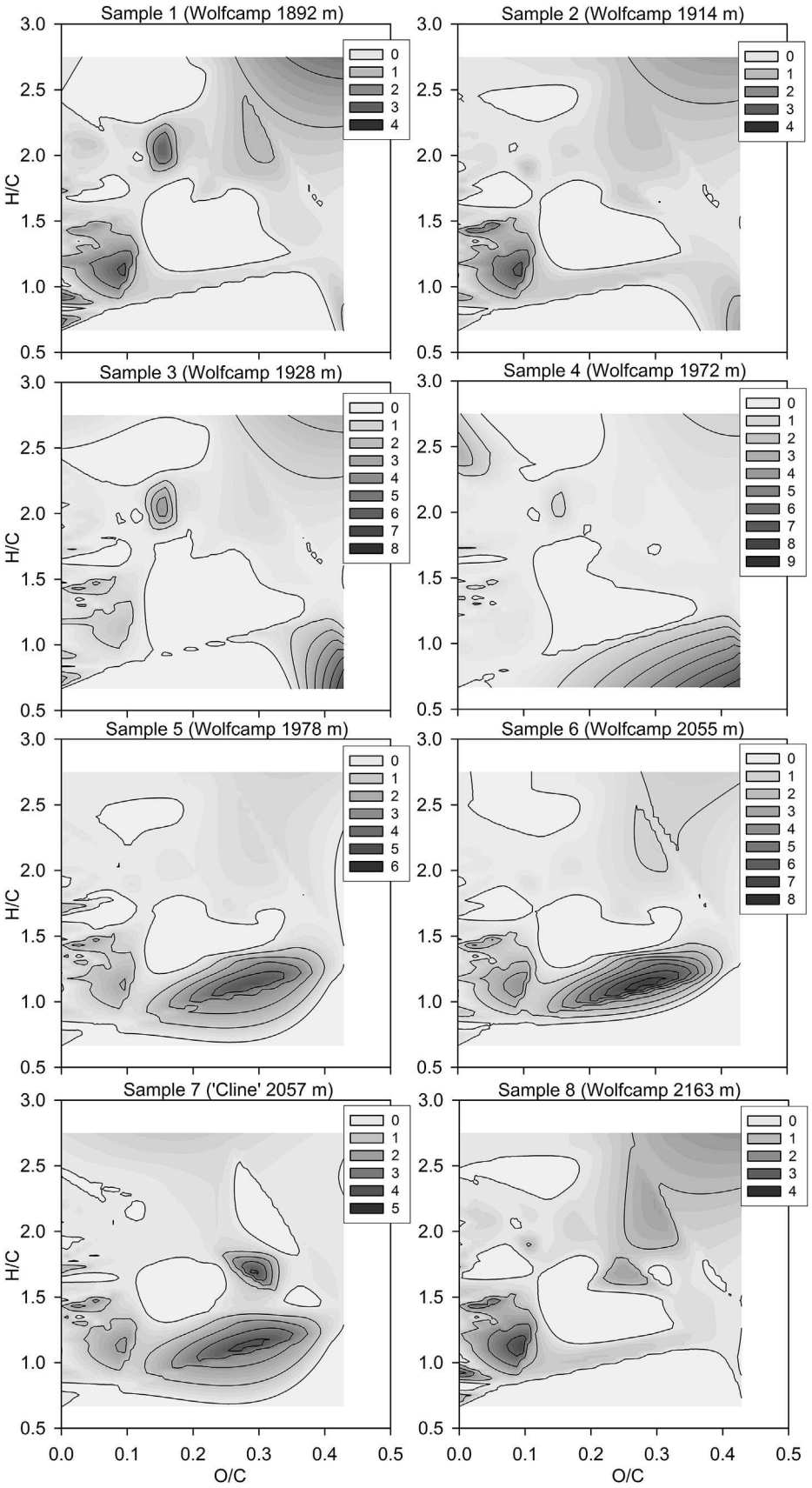

Fig. 5. Comparison of 3D van Krevelen (H/C versus O/C) with relative abundance (%) contours. Plots increase in sampled formation depth from left to right and top to bottom.

Table 3
Summary of abundance peak compounds (and their molar ratios) identified on van Krevelen and double-bond equivalent (DBE) versus carbon plots.

H/C	O/C	Compound name	Formula	CAS
2.8	0.3	Hydroxylamine, O-(2-methylpropyl)	$C_4H_{11}NO$	5618-62-2
2.3	0.1	Nitroxide, bis(1,1-dimethylethyl)	$C_8H_{18}NO$	2406-25-9
1.2	0.1	Ethanone, 1-(2,4-dimethylphenyl)-	$C_{10}H_{12}O$	89-74-7
2.4	0.0	Pentane	C_5H_{12}	109-66-0
1.3	0.4	3-Butene-1,2-diol, 1-(2-furanyl)	$C_8H_{10}O_3$	19261-13-3
1.4	0.0	Benzene, 1-methyl-3-propyl-	$C_{10}H_{14}$	1074-43-7
1.7	0.3	Acetyl valeryl	$C_7H_{12}O_2$	96-04-8
H/C	**N/C**	**Compound name**	**Formula**	
1.7	0.3	Butanenitrile	C_4H_7N	109-74-0
1.8	0.3	Cyanic acid, propyl ester	C_4H_7NO	1768-36-1
1.7	0.3	2,3-Diazabicyclo[2.2.1]hept-2-ene, 1,4-dimethyl-	$C_7H_{12}N_2$	71312-54-4
DBE	**C**	**Compound name**	**Formula**	
10	14	Phenanthrene	$C_{14}H_{10}$	85-01-8
7	14	1,4,5,8-Tetramethylnaphthalene	$C_{14}H_{16}$	2717-39-7
7	11	Naphthalene, 2-methyl-	$C_{11}H_{10}$	91-57-6
4	10	Benzene, 1-methyl-3-propyl-	$C_{10}H_{14}$	1074-43-7
5	10	Ethanone, 1-(2,4-dimethylphenyl)-	$C_{10}H_{12}O$	89-74-7
2	4	Butanenitrile	C_4H_7N	109-74-0
3	6	2-methoxyfuran	$C_5H_6O_2$	25414-22-6
4	6	Benzene	C_6H_6	71-43-2
4	9	Benzene, propyl-	C_9H_{12}	103-65-1
2	7	3-methylcyclohexene	C_7H_{12}	591-48-0

PW from oil production in Wyoming, which ranged from DBE 0-16 and C 6-25 with increased abundance from DBE 2-4 and C 10-15 (Wang et al., 2012).

Higher DBE values indicate greater aromaticity and less hydrogen saturation. Cho et al. determined that DBE values for shale-oil ranged between 4 and 7 as determined using FT-ICR-MS, and they found that shale-oil had a lower range of DBE relative to oil (Cho et al., 2013). DBE plots ranged from DBE 10-20 with C 25-50 for oil and ranged from DBE 5-25 with C 10-60 for gas-oil cuts (Stanford et al., 2007; Avila et al., 2012). The results for PW from shale-oil in the Permian Basin had dominant organic compounds with DBE values ranging from 2 to 8 (Fig. 7), which is comparable to the range for shale-oil (Cho et al., 2013). These results also support the observation that source-oil composition has a significant impact on PW composition. However, they also suggest solubility controls constrain PW composition. For example, low-solubility asphaltenes are typical constituents of petroleum that have DBE values generally higher (20–35) than byproducts of petroleum such as PWs (Wang et al., 2012). As noted for the van Krevelen evaluation, 3D DBE versus carbon number fingerprinting (another petroleomics evaluation) can also be used to characterize PW from oil and gas production including shale-oil. Both 3D van Krevelen and DBE plots provide additional mixture characterization information, and used together these provide a fingerprinting framework for high-resolution MS analysis results.

4. Conclusions

This study characterized the volatile organic compositional variability of late stage shale-oil PW from the Permian Basin. Benzene, and other BTEX compounds, are of significant concern for risk to human health and environment, and these compounds are elevated above drinking water and irrigation water quality standards. For beneficial use of the water, the organic contaminants must be removed from PWs (Xu et al., 2008a; Graham et al., 2015). Although not the focus of this work, several metals and anions had concentration ranges that exceeded drinking water or irrigation standards (i.e., B, Ba, Be, Ca, Cd, Cu, Fe, K, Li, Mg, Mn, Se, and Cl) (data not shown). However, for shale-oil PW the extremely elevated TDS represents the primary challenge for water treatment and reuse. The results presented herein suggest that partial treatment by removing suspended solids and organic contaminants would support some beneficial uses such as onsite reuse (e.g., hydraulic fracturing), bio-energy production, and mining (Xu et al., 2008a; Graham et al., 2015). Since potable water is still widely used for hydraulic fracturing, replacing potable water with partially-treated PW for hydraulic fracturing operations is one industrial reuse option that may be viable, and this would support water resource sustainability especially in water scarce arid regions such as the Permian Basin. However, minimization of compositional variability may be required for fracturing operations.

The compositional variability of volatile organics in shale-oil PW of the Permian Basin was evaluated through high-resolution molecular characterization using GC-ToF-MS and petroleomics evaluation techniques. As a lower-cost alternative to FT-ICR-MS, GC-ToF-MS provided high-resolution identification for the semivolatile and volatile compounds, which may be the greatest concern for PW and potentially associated environmental impacts. Approximately 1400 organic chemicals were observed with 300–400 identifiable structures, which fills a data gap for shale-oil PW. Shale-oil PW was found to be an extremely complex organic mixture for natural waters such that high-resolution MS was required to quantify the variability. The results suggest that the volatile organic compositional complexity may be used to fingerprint PW for forensic evaluations. However, this study was limited, and further evaluation is needed for different formations and types of PW. van Krevelen and DBE versus carbon number diagrams were used to evaluate composition patterns and variability, and used together these provide a fingerprinting framework for high-resolution MS analysis results. Such evaluation supports examination of potential environmental impacts for PW spills, beneficial use, or reuse alternatives. Treatment design also may be supported by high-resolution compositional analysis. Both shale-oil PWs and shale-oil have elevated alkanes compared to cyclohexane, cyclopentane, and naphthalene, and both are also dominated by N_1, N_2, N_1O_1, and O_2 containing heteroatomic compound classes, which confirms source oil control over shale-oil PW composition. Additionally, solubility and inorganic composition tends to impact dissolution

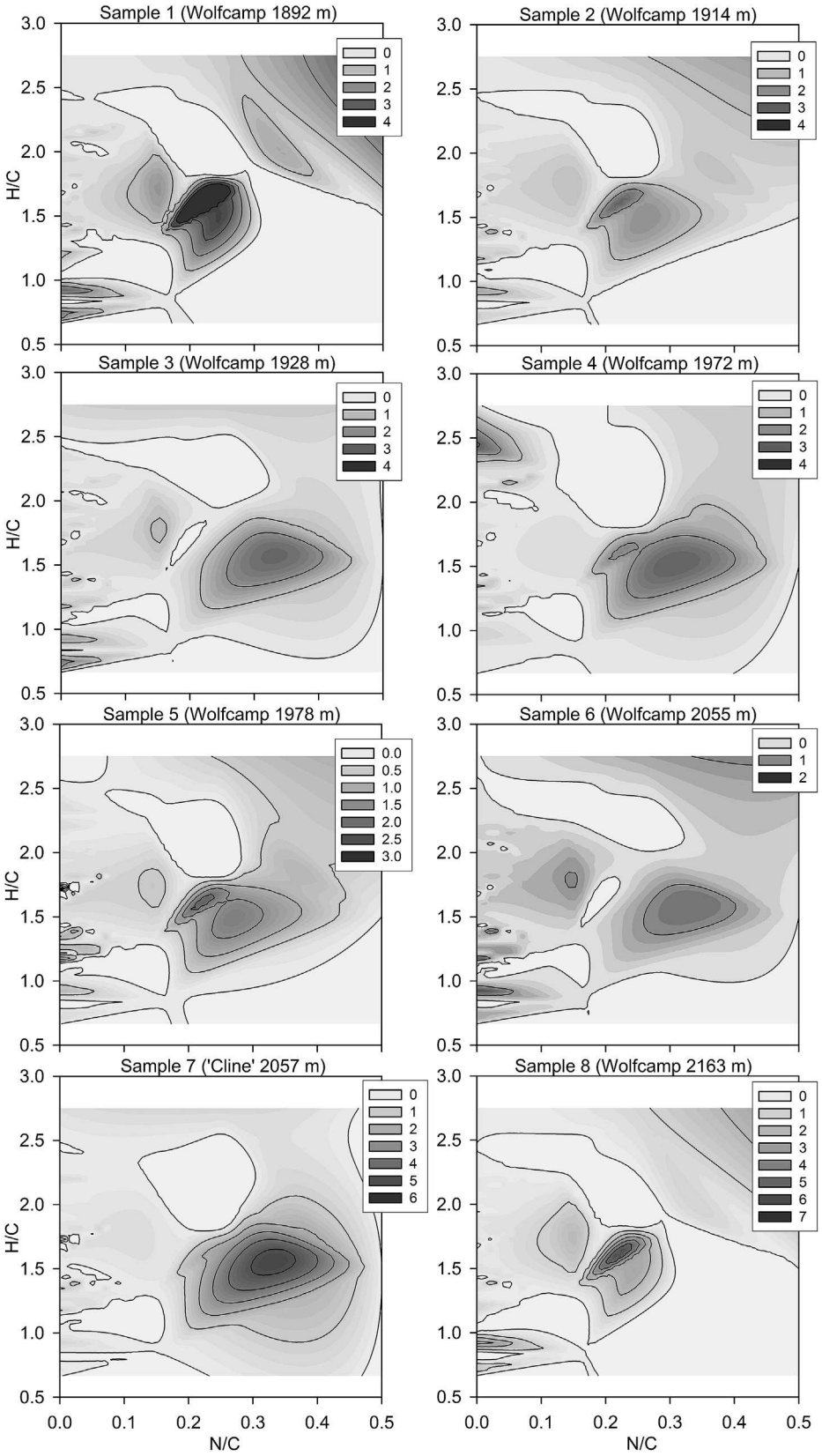

Fig. 6. Comparison of 3D van Krevelen (H/C versus N/C) with relative abundance (%) contours. Plots increase in sampled formation depth from left to right and top to bottom.

from shale-oil into PW. Moreover, molecular techniques have been shown to contribute tremendous information for characterization of complex organic mixtures such as PW, and high-resolution molecular characterization can be used to support evaluation of

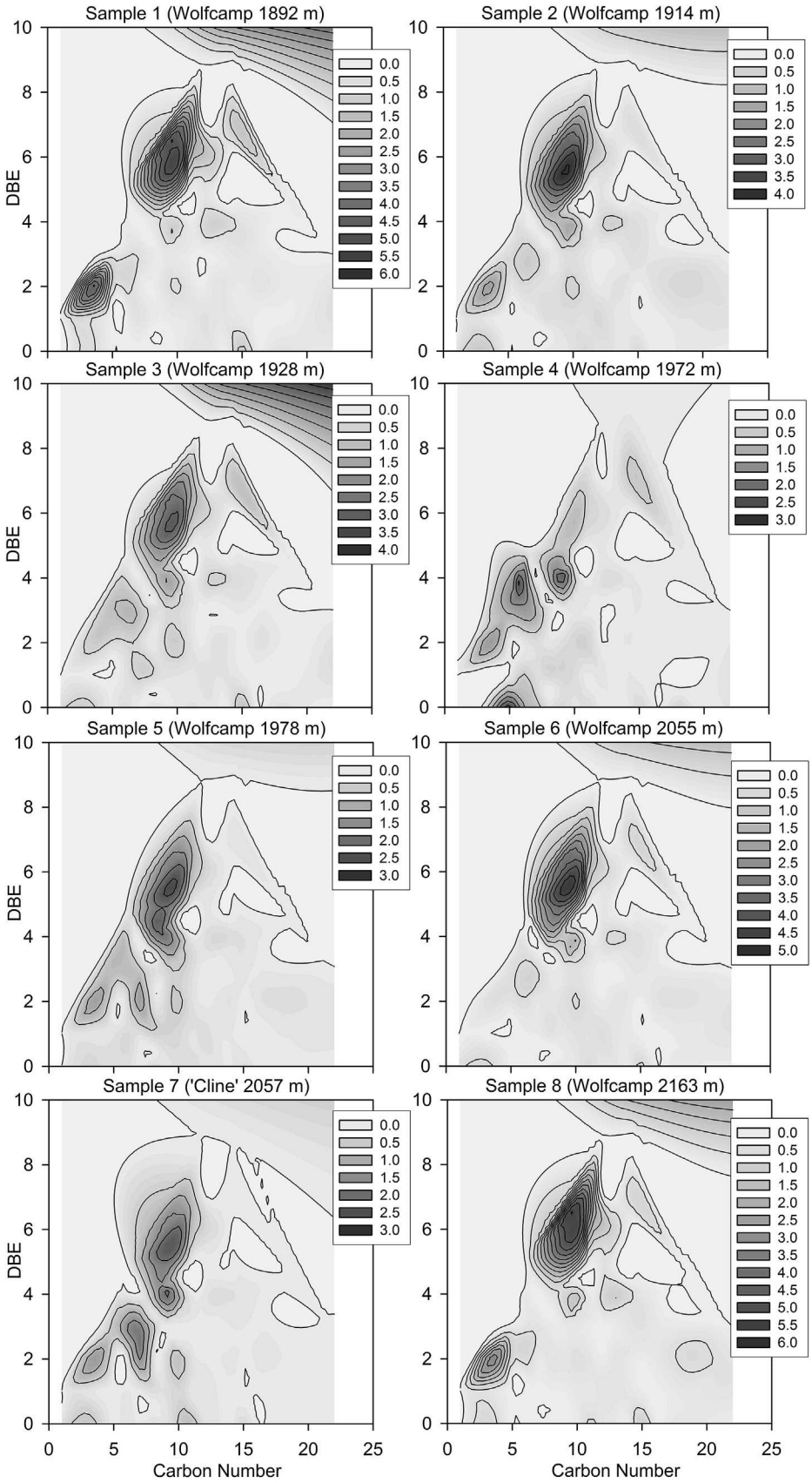

Fig. 7. Comparison of 3D double bond equivalence (DBE) versus carbon with relative abundance (%) contours. Plots increase in depth from left to right and top to bottom.

beneficial use options and treatment needs of PW.

Acknowledgments

This work was supported by the New Mexico State University Office of the Vice President for Research, the U.S. Geological Survey Energy Resources Program, and the Research Partnership to Secure Energy for America (Subcontract #11122-53). Anonymous reviewer comments were appreciated and improved the clarity of this work. The authors would like to thank the numerous oil and gas operators that provided access to sample their wells, valuable insight into their operations, and necessary data. We also thank Barbara Hunter, Nilusha Appuhamilage, and Zack Stoll for their assistance. Disclaimer — use of trade or product names is for descriptive purposes only and does not imply endorsement by the U.S. Government.

References

Ahmadun, F.R., Pendashteh, A., Abdullah, L.C., Biak, D.R.A., Madaeni, S.S., Abidin, Z.Z., 2009. Review of technologies for oil and gas produced water treatment. J. Hazard. Mater. 170, 530–551.

Alley, B., Beebe, A., Rodgers, J., Castle, J.W., 2011. Chemical and physical characterization of produced waters from conventional and unconventional fossil fuel resources. Chemosphere 85, 74–82.

Avila, B.M.F., Vaz, B.G., Pereira, R., Gomes, A.O., Pereira, R.C.L., Corilo, Y.E., Simas, R.C., Nascimento, H.D.L., Eberlin, M.N., Azevedo, D.A., 2012. Comprehensive chemical composition of gas oil cuts using two-dimensional gas chromatography with time-of-flight mass spectrometry and electrospray ionization coupled to Fourier transform ion cyclotron resonance mass spectrometry. Energy & Fuels 26, 5069–5079.

Bassett, R.L., Bentley, M.E., 1982. Geochemistry and hydrodynamics of deep formation brines in the Palo Duro and Dalhart basins, Texas, USA. J. Hydrol. 59, 331–372.

Cho, Y., Jin, J.M., Witt, M., Birdwell, J.E., Na, J.G., Roh, N.S., Kim, S., 2013. Comparing laser desorption ionization and atmospheric pressure photoionization coupled to Fourier transform ion cyclotron resonance mass spectrometry to characterize shale oils at the molecular level. Energy & Fuels 27, 1830–1837.

Cho, Y.J., Na, J.G., Nho, N.S., Kim, S., Kim, S., 2012. Application of saturates, aromatics, resins, and asphaltenes crude oil fractionation for detailed chemical characterization of heavy crude oils by Fourier transform ion cyclotron resonance mass spectrometry equipped with atmospheric pressure photoionization. Energy & Fuels 26, 2558–2565.

Dorea, H.S., Bispo, J.R.L., Aragao, K.A.S., Cunha, B.B., Navickiene, S., Alves, J.P.H., Romao, L.P.C., Garcia, C.A.B., 2007. Analysis of BTEX, PAHs and metals in the oilfield produced water in the state of Sergipe, Brazil. Microchem. J. 85, 234–238.

Dudasova, D., Flaten, G.R., Sjoblom, J., Oye, G., 2009. Stability of binary and ternary model oil-field particle suspensions: a multivariate analysis approach. J. Colloid Interface Sci. 337, 464–471.

Dutton, A.R., 1987. Origin of brine in the San-Andres formation, evaporite confining system, Texas Panhandle and eastern New Mexico. Geol. Soc. Am. Bull. 99, 103–112.

Dutton, S.P., Kim, E.M., Broadhead, R.F., Raatz, W.D., Breton, C.L., Ruppel, S.C., Kerans, C., 2005. Play analysis and leading-edge oil-reservoir development methods in the Permian basin: increased recovery through advanced technologies. AAPG Bull. 89, 553–576.

Eftekhardadkhah, M., Oye, G., 2013. Correlations between crude oil composition and produced water quality: a multivariate analysis approach. Ind. Eng. Chem. Res. 52, 17315–17321.

Engle, M.a., Blondes, M.S., 2014. Linking compositional data analysis with thermodynamic geochemical modeling: oilfield brines from the Permian Basin, USA. J. Geochem. Explor. 141, 61–70.

Faksness, L.G., Grini, P.G., Daling, P.S., 2004. Partitioning of semi-soluble organic compounds between the water phase and oil droplets in produced water. Mar. Pollut. Bull. 48, 731–742.

Franson, M.A.H. (Ed.), 1992. Standard Methods for the Examination of Water and Wastewater. American Public Health Association, Washington, DC.

Graham, E.J.S., Jakle, A.C., Martin, F.D., 2015. Reuse of oil and gas produced water in south-eastern New Mexico: resource assessment, treatment processes, and policy. Water Int. 40, 809–823.

Guerra, K., Dahm, K., Dundorf, S., 2011. Oil and Gas Produced Water Management and Beneficial Use in the Western United States. U.S. Department of the Interior Bureau of Reclamation Denver, Colorado.

Horner, J.E., Castle, J.W., Rodgers, J.H., 2011. A risk assessment approach to identifying constituents in oilfield produced water for treatment prior to beneficial use. Ecotoxicol. Environ. Saf. 74, 989–999.

Jin, J.M., Kim, S., Birdwell, J.E., 2012. Molecular characterization and comparison of shale oils generated by different pyrolysis methods. Energy & Fuels 26, 1054–1062.

Kekalainen, T., Pakarinen, J.M.H., Wickstrom, K., Lobodin, V.V., McKenna, A.M., Janis, J., 2013. Compositional analysis of oil residues by ultrahigh-resolution Fourier transform ion cyclotron resonance mass spectrometry. Energy & Fuels 27, 2002–2009.

Kim, S., Kramer, R.W., Hatcher, P.G., 2003. Graphical method for analysis of ultrahigh-resolution broadband mass spectra of natural organic matter, the van Krevelen diagram. Anal. Chem. 75, 5336–5344.

Lababidi, S., Panda, S.K., Andersson, J.T., Schrader, W., 2013. Deep well deposits: effects of extraction on mass spectrometric results. Energy & Fuels 27, 1236–1245.

Lambropoulou, D.A., Albanis, T.A., 2001. Optimization of headspace solid-phase microextraction conditions for the determination of organophosphorus insecticides in natural waters. J. Chromatogr. A 922, 243–255.

Lu, J.R., Wang, X.L., Shan, B.T., Li, X.M., Wang, W.D., 2006. Analysis of chemical compositions contributable to chemical oxygen demand (COD) of oilfield produced water. Chemosphere 62, 322–331.

Maguire-Boyle, S.J., Barron, A.R., 2014. Organic compounds in produced waters from shale gas wells. Environ. Sci. Processes Impacts 16, 2237–2248.

Orem, W., Tatu, C., Varonka, M., Lerch, H., Bates, A., Engle, M., Crosby, L., McIntosh, J., 2014. Organic substances in produced and formation water from unconventional natural gas extraction in coal and shale. Int. J. Coal Geol. 126, 20–31.

Ostroff, A.G., 1979. Introduction to Oilfield Water Technology. National Association of Corrosion Engineers, Houston (Texas).

Rowan, E.L., Engle, M.A., Kraemer, T.F., Schroeder, K.T., Hammack, R.W., Doughten, M.W., 2015. Geochemical and isotopic evolution of water produced from middle Devonian Marcellus shale gas wells, Appalachian basin, Pennsylvania. AAPG Bull. 99, 181–206.

Senger, R.K., Kreitler, C.W., Fogg, G.E., 1987. Regional underpressuring in deep brine aquifers, Palo-Duro Basin, Texas .2. The effect of Cenozoic Basin development. Water Resour. Res. 23, 1494–1504.

Silset, A., Flaten, G.R., Helness, H., Melin, E., Oye, G., Sjoblom, J., 2010. A multivariate analysis on the influence of indigenous crude oil components on the quality of produced water. Comparison between bench and Rig scale experiments. J. Dispers. Sci. Technol. 31, 392–408.

Sirivedhin, T., Dallbauman, L., 2004. Organic matrix in produced water from the Osage-Skiatook petroleum environmental research site, Osage County, Oklahoma. Chemosphere 57, 463–469.

Stanford, L.A., Rodgers, R.P., Marshall, A.G., Czarnecki, J., Wu, X.A., Taylor, S., 2007. Detailed elemental compositions of emulsion interfacial material versus parent oil for nine geographically distinct light, medium, and heavy crude oils, detected by negative- and positive-ion electrospray ionization Fourier transform ion cyclotron resonance mass spectrometry. Energy & Fuels 21, 973–981.

Tellez, G.T., Nirmalakhandan, N., Gardea-Torresdey, J.L., 2005. Comparison of purge and trap GC/MS and spectrophotometry for monitoring petroleum hydrocarbon degradation in oilfield produced waters. Microchem. J. 81, 12–18.

U.S.E.I.A, 2015. Drilling Productivity Report U.S. Energy Information Administration. http://www.eia.gov/petroleum/drilling/#tabs-summary-2.

Utvik, T.I.R., 1999. Chemical characterisation of produced water from four offshore oil production platforms in the North Sea. Chemosphere 39, 2593–2606.

Veil, J., Puder, M., Elcock, D., Redweik Jr., R., 2004. A White Paper Describing Produced Water from Production of Crude Oil, Natural Gas, and Coal Bed Methane. U.S. Department of Energy, National Energy Technology Laboratory.

Wang, X.J., Goual, L., Colberg, P.J.S., 2012. Characterization and treatment of dissolved organic matter from oilfield produced waters. J. Hazard. Mater. 217, 164–170.

Wu, Z.G., Rodgers, R.P., Marshall, A.G., 2004. Two- and three-dimensional van Krevelen diagrams: a graphical analysis complementary to the Kendrick mass plot for sorting elemental compositions of complex organic mixtures based on ultrahigh-resolution broadband Fourier transform ion cyclotron resonance mass measurements. Anal. Chem. 76, 2511–2516.

Xu, P., Drewes, J.E., Heil, D., 2008a. Beneficial use of co-produced water through membrane treatment: technical-economic assessment. Desalination 225, 139–155.

Xu, P., Drewes, J.E., Heil, D., Wang, G., 2008b. Treatment of brackish produced water using carbon aerogel-based capacitive deionization technology. Water Res. 42, 2605–2617.

Zhou, B., Xiao, J.F., Tuli, L., Ressom, H.W., 2012. LC-MS-based metabolomics. Mol. Biosyst. 8, 470–481.